SANDIA REPORT
SAND2016-0696
Unlimited Release
January 2016

Coupling a Supercritical Carbon Dioxide Brayton Cycle to a Helium-Cooled Reactor

Bobby D. Middleton, James R. Pasch, Alan, Kruizenga, Matthew Walker

Prepared by
Sandia National Laboratories
Albuquerque, New Mexico 87185 and Livermore, California 94550

Sandia National Laboratories is a multi-program laboratory managed and operated by Sandia Corporation, a wholly owned subsidiary of Lockheed Martin Corporation, for the U.S. Department of Energy's National Nuclear Security Administration under contract DE-AC04-94AL85000.

Issued by Sandia National Laboratories, operated for the United States Department of Energy by Sandia Corporation.

Printed in the United States of America. This report has been reproduced directly from the best available copy.

Available to DOE and DOE contractors from
U.S. Department of Energy
Office of Scientific and Technical Information
P.O. Box 62
Oak Ridge, TN 37831

Telephone: (865) 576-8401
Facsimile: (865) 576-5728
E-Mail: reports@osti.gov
Online ordering: http://www.osti.gov/scitech

Available to the public from
U.S. Department of Commerce
National Technical Information Service
5301 Shawnee Rd
Alexandria, VA 22312

Telephone: (800) 553-6847
Facsimile: (703) 605-6900
E-Mail: orders@ntis.gov
Online order: http://www.ntis.gov/search

SAND2016-0696
Unlimited Release
January 2016

Coupling a Supercritical Carbon Dioxide Brayton Cycle to a Helium-Cooled Reactor

Bobby Middleton
James Pasch
Advanced Nuclear Concepts
Sandia National Laboratories
P.O. Box 5800
Mail Stop 1136
Albuquerque, New Mexico 87185-MS1136

Alan Kruizenga
Matthew Walker
Materials Chemistry
Sandia National Laboratories
P.O. Box 969
Mail Stop9403
Livermore, CA 94551 -MS9403

ABSTRACT

This report outlines the thermodynamics of a supercritical carbon dioxide (sCO_2) recompression closed Brayton cycle (RCBC) coupled to a Helium-cooled nuclear reactor. The baseline reactor design for the study is the AREVA High Temperature Gas-Cooled Reactor (HTGR). Using the AREVA HTGR nominal operating parameters, an initial thermodynamic study was performed using Sandia's deterministic RCBC analysis program. Utilizing the output of the RCBC thermodynamic analysis, preliminary values of reactor power and of Helium flow rate through the reactor were calculated in Sandia's HelCO2 code. Some research regarding materials requirements was then conducted to determine aspects of corrosion related to both Helium and to sCO_2, as well as some mechanical considerations for pressures and temperatures that will be seen by the piping and other components. This analysis resulted in a list of materials-related research items that need to be conducted in the future. A short assessment of dry heat rejection advantages of sCO_2 Brayton cycles was also included. This assessment lists some items that should be investigated in the future to better understand how sCO_2 Brayton cycles and nuclear can maximally contribute to optimizing the water efficiency of carbon free power generation

CONTENTS

FIGURES

TABLES

1. INTRODUCTION

The Department of Energy, Office of Nuclear Energy (DOE-NE) has funded a study to determine the characteristics of a high-temperature test reactor. The Idaho National Laboratory (INL) is developing a report that will describe a High-Temperature Gas-cooled Reactor (HTGR). As part of the study supporting this report, INL requested that Sandia National Laboratories (SNL) write a report discussing the major points of emphasis for coupling such a reactor to supercritical carbon dioxide Brayton cycle for power conversion. This report completes that request. The report covers three broad areas.

- Preliminary power conversion trade study: This section of the report covers results of a study that varied the two most impactful parameters of the Recompression Closed Brayton Cycle (RCBC), which are the turbine inlet temperature and cycle maximum pressure. It was assumed for this study that the electrical output of the system would be held constant at 250 MWe. The outputs of the study are plots of cycle thermal efficiency, sCO_2 mass flow rate, intermediate heat exchanger inlet temperature, reactor power, and Helium mass flow rate.
- Materials considerations: This section of the report covers the results of a literature review of some materials considerations that should be considered when assessing a HTGR that utilizes a sCO_2 Brayton cycle for power conversion.
- Dry heat rejection: This section of the report discusses some ways in which the sCO_2 Brayton cycle could aid in drastically reducing the amount of water needed to produce electricity by utilizing dry heat rejection technologies to replace wet cooling technologies.

2. BRAYTON CYCLE

The term "Brayton Cycle" refers to a family of thermodynamic cycles wherein the working fluid stays in a single, gaseous phase as it is heated and cooled [1]. The cycle chosen for this study is a Recompression Closed Brayton Cycle (RCBC). This cycle achieves a very high degree of internal heat recuperation. Much work at Sandia National Laboratories (SNL) and other research institutions indicates that the relative thermal efficiency and cost of such a cycle make it the best option for near-term investment in power conversion cycles.

A major factor of plant installed cost is plant size, which correlates strongest with power level. Trade studies of sCO_2 RCBCs show that plant size, and therefore installed costs, also correlates strongly with conversion cycle maximum pressure through the CO_2 mass flow rate. The maximum pressure, or pressure ratio, also directly affects conversion efficiency, which affects operating costs. Figure 1 shows this relationship.

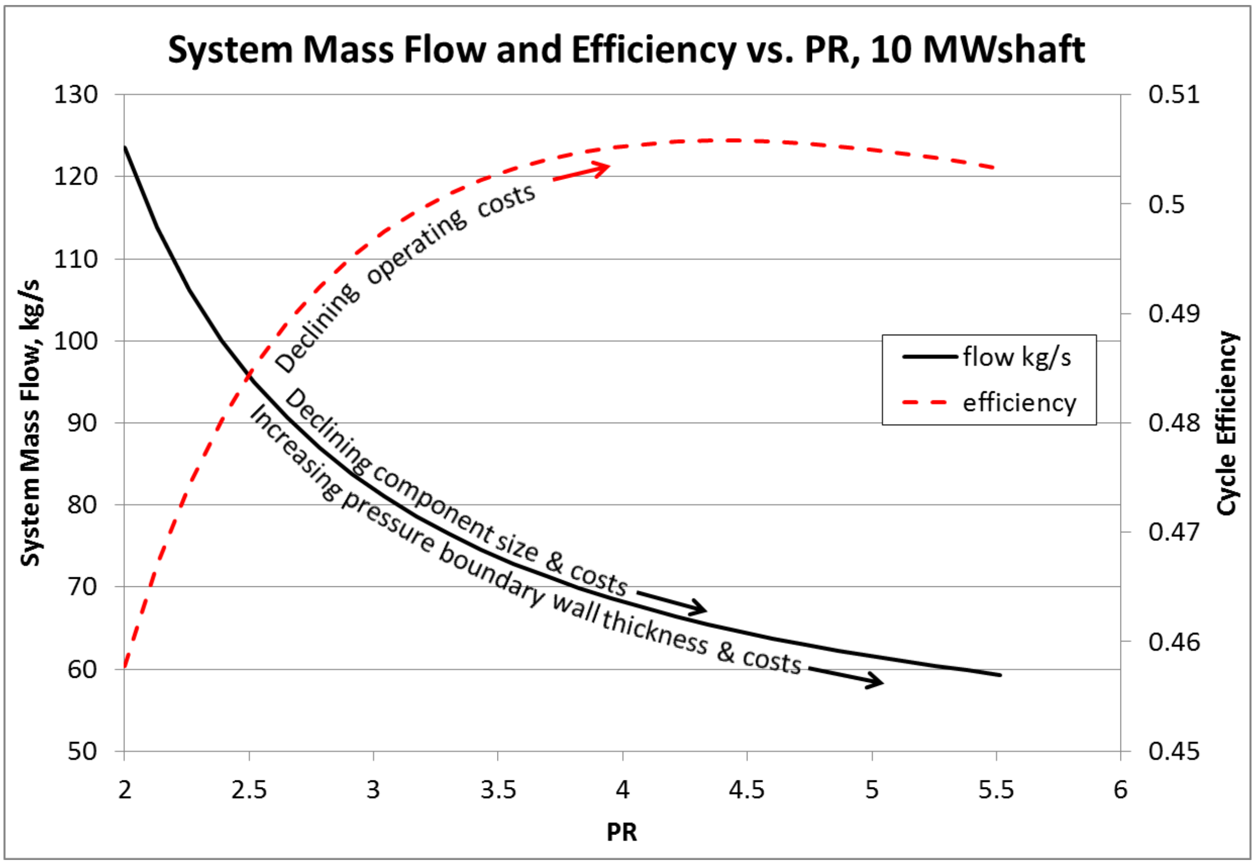

Figure 1: Relation of system mass flow and efficiency with compressor pressure ratio.

Piping and component sizes, and therefore costs, correlate strongly with the amount of material used, and costs of major components such as recuperators and valves are additionally affected by construction time. Using PCHE recuperators as an example, construction size, and therefore cost, is directly affected by the size and number of shims necessary to accommodate the flow. Shim flow path etching, which is the most costly part of manufacture, and diffusion bonding of shims, are both directly affected by the number and size of shims. Header weldments increase in size as the recuperator size increases.

A detriment to plant cost of raising system pressure is a necessary increase in piping and component wall thicknesses to accommodate the associated higher pressure differentials. For piping, this effect is largely confined to simply designing to avoid ruptures. The detriment is exacerbated and more complicated for heat exchangers since larger wall thicknesses degrade heat transfer performance. The search for the optimal solution is a complex relationship that quantifies these various engineering performance characteristics and their associated effects on installed and operating costs. Figure 2 below gives the trend relationship between the engineering considerations of system pressure and the economics quantified in levelized cost of energy (LCOE).

Projecting installed costs, which correlates with mass flow, may have less uncertainty as the time frame is nearer term and material and construction costs are likely better understood. Projecting operating costs and associated cash flows over a period of years, which correlates with conversion efficiency, has significantly greater uncertainty.

The remaining analyses will focus more on the engineering aspects of the HTGR and less on the economics. However, it is recommended that the reader remain cognizant of the relationships between engineering performance and LCOE that have been presented above.

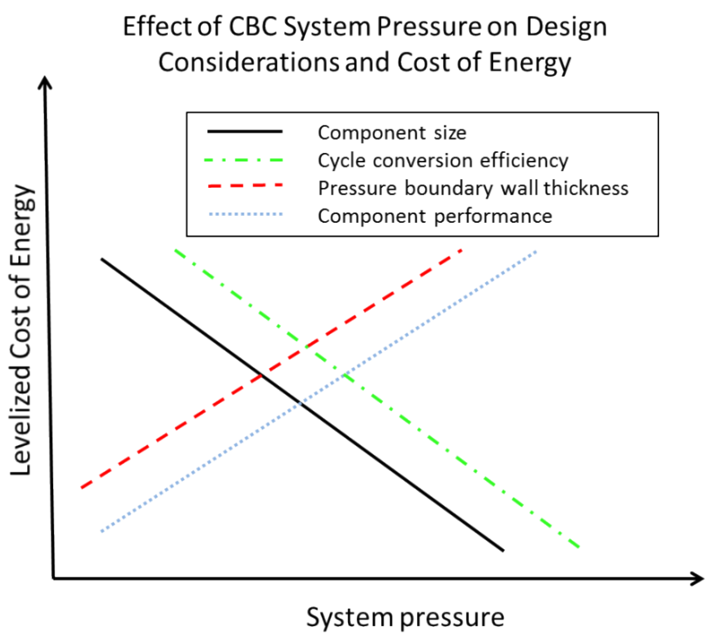

Figure 2: Effect of maximum system pressure on various factors of LCOE.

Projecting installed costs, which correlates with mass flow, may have less uncertainty as the time frame is nearer term and material and construction costs are likely better understood. Projecting operating costs and associated cash flows over a period of years, which correlates with conversion efficiency, has significantly greater uncertainty.

The remaining analyses will focus more on the engineering aspects of the HTGR and less on the economics. However, it is recommended that the reader remain cognizant of the relationships between engineering performance and LCOE that have been presented above.

This page intentionally left blank.

3. POWER CONVERSION CYCLE PERFORMANCE FOR THE HTGR

Nominal Configuration Assessment of Brayton Cycle

The preferred power conversion cycle for a closed heat source, such as a nuclear reactor or a concentrated solar power system, is the recompression closed Brayton cycle (RCBC). This is because of the very high degree of cycle internal heat recuperation that is achieved with the high and low temperature recuperators (HTR, LTR). The result of this extensive reclamation of turbine discharge heat is a hot process flow that enters the primary heat source. This hot sCO2 cannot decrease the heat source flow temperature below the sCO2 inlet temperature. Thus, a great deal of heat energy remains in the heat source flow. In a closed heat source, this does not matter. However, in an open heat source, the result is either a great reduction in conversion performance if it is expelled as waste heat, or the implementation of a bottoming cycle and associated costs to make use of the remaining heat.

To model the RCBC in a deterministic program, a number of thermodynamic and performance conditions must be set by the user of the program. In the program developed at SNL, ten conditions were selected. The thermodynamic cycle and selected conditions are presented in the Figure 3. The green boxes indicate which parameters are the control parameters, and the definitions of these parameters are given in the box in this figure. For the studies that follow, the values set for these parameters are given in tables. The most important controls are the main compressor inlet pressure and temperature, which may vary between studies in order to maximize predicted performance.

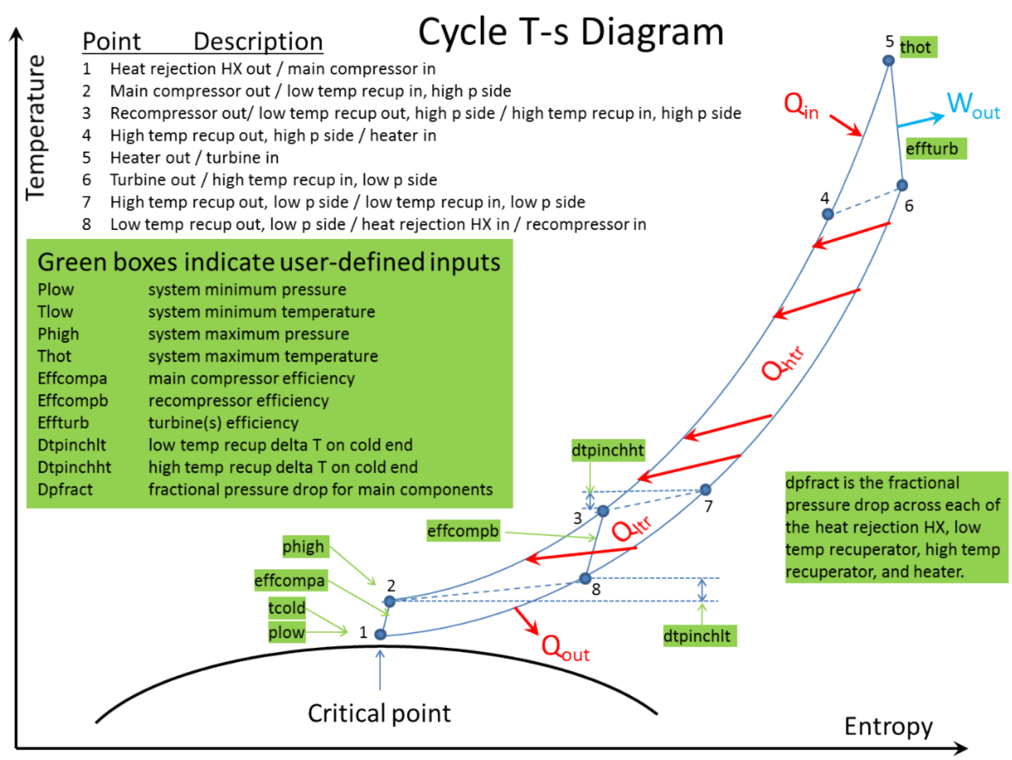

Figure 3: T-S diagram for the RCBC, and control parameters used to close out set of equations in the program.

Nominal values were based on a combination of the Table 1, taken from literature on the AREVA HTGR, commonly accepted values for component performance, and optimal values for the RCBC in relation to this HTGR. The 250 MWe power output represents 50% cycle conversion efficiency after an intermediate heat exchanger (IHX) efficiency of 80%[1]. In other words, 250 MWe = 625 MWth * η_{IHX} * η_{cycle}. It must be remembered that this is a nominal electrical power level, and that each study will have somewhat different outputs, but for the intention of performing general trade studies, this approach is adequate. The 658 °C represents the average between the reactor discharge temperature and the steam temperature. 25 MPa cycle pressure is a commonly used value. Turbine and compressor efficiencies of 90% and 80% are deemed reasonable for near term goals by turbomachinery vendors. The high and low temperature recuperator pinch temperatures of 20 °C and 10 °C come from the design performance of the SNL RCBC PCHE's. The 1% pressure drop at each component also is a design parameter of the SNL RCBC. For these conditions, the optimal sCO2 thermodynamic state at the compressor inlet is roughly 32 °C and 7.7 MPa.

Table 1 Operating conditions for the AREVA HTGR that is presented in [2].

Fuel type	TRISO Coated Particle
Core geometry	102 column annular 10 blocks high
Reactor power	625 MWt
Reactor outlet temperature	750°C (1382°F)
Reactor inlet temperature	325°C (617°F)
Primary coolant pressure	6 MPa (870 psia)
Vessel Material	SA 508/533
Number of loops	2
Steam generator power	315 MWt (each)
Main circulator power	4 MWe (each)
Main steam temperature	566°C (1050°F)
Main steam pressure	16.7 MPa (2422 psia)

[1] 80% is on the low end of values that should be used. It is expected that IHX effectiveness should be between 85% and 95%. However, for an initial study with the purpose of finding trends and estimated values, 80% works well.

Table 2 Nominal values used in trade studies of the RCBC for the HTGR.

Parameter	Units	Value
Main compressor inlet temperature	°C	32
Main compressor inlet pressure	MPa	7.7
Compressor discharge pressure	MPa	25
Turbine inlet temperature	°C	658
Low temp recuperator pinch temp at cold end	Δ°C	10
High temp recuperator pinch temp at cold end	Δ°C	20
Turbine efficiency	-	0.90
Main compressor efficiency	-	0.80
Recompressor efficiency	-	0.80
Fractional pressure drop through each major component	ΔP/P	0.01
Electric Power Output	MWe	250

The RCBC flow sheet for these specific conditions is presented in Figure 4. Recuperator size is based on SNL PCHE duty and sizing information.

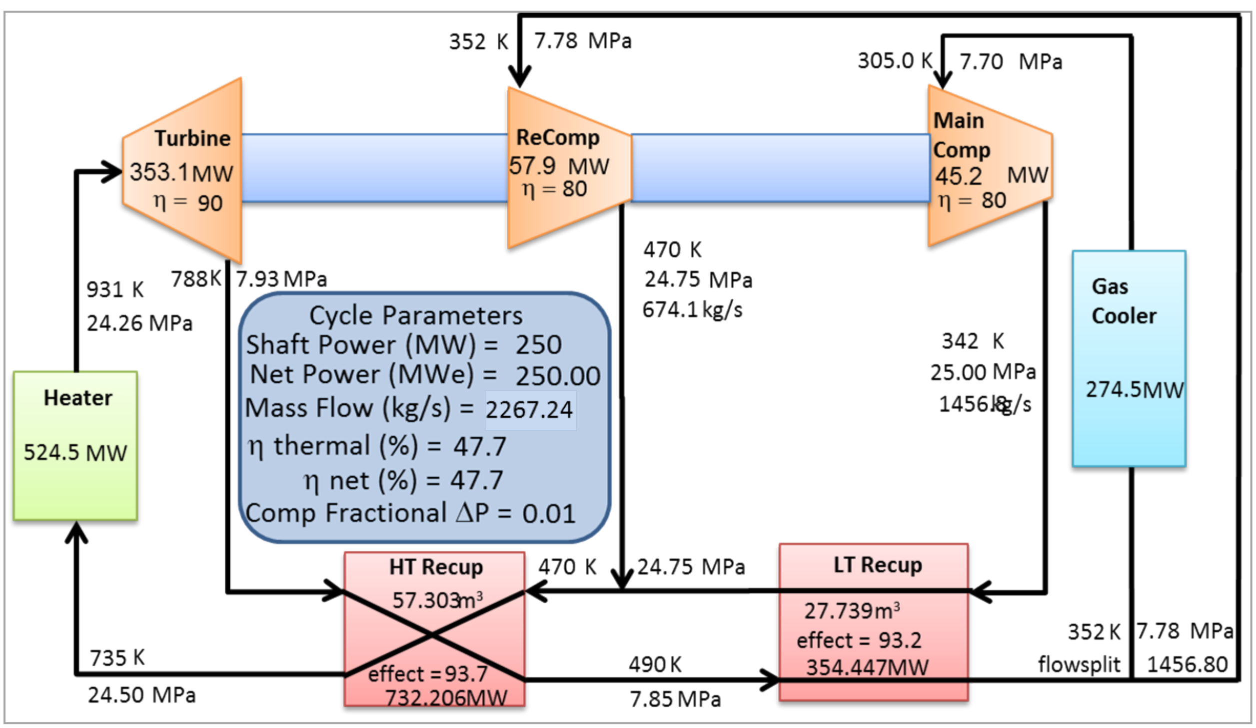

Figure 4 Flow sheet for RCBC operating at nominal conditions for this study.

Nominal Configuration Assessment of HTGR

Using the output from the RCBC analysis, an energy balance calculation was performed to determine the required reactor power and the Helium flow rate required to produce the 524.5 MWth transferred to the sCO_2 power conversion system. The assumptions used and the output are presented in Table 3. The outputs are reactor power and helium flow rate; they are written in bold text in Table 3.

Table 3 Parameters used and results from calculating required reactor power and Helium flow rate for Nominal Configuration.

Parameter	Units	Value
IHX Effectiveness	-	0.80
Thermal Efficiency	-	0.4766
Rx Exit Temperature	°C	673
Reactor Inlet Temperature	°C	477
Reactor Max Pressure	MPa	6.00
Reactor dP/P	-	0.05
Reactor Power	**MW**	**655.6**
Helium Flow Rate	**kg/sec**	**645.1**

Sensitivity Assessment of Brayton Cycle Control Parameters

To analyze the effect of the most important control parameters in the RCBC, the compressor discharge pressure (Cycle Maximum Pressure) and the turbine inlet temperature were varied. The range of pressures was from 20 MPa to 35 MPa, in 0.5 MPa increments. The turbine inlet temperatures ranged from 550 °C to 750 °C, in 10 °C increments.

For this study, Table 4 gives the input conditions. As expected and shown in Figure 5, efficiency increases strongly with turbine inlet temperature, and less strongly with maximum pressure. Mass flow rate necessary to achieve the specified power level, shown in Figure 6, declines as turbine inlet temperature and system pressure increase. Figure 7 shows that the temperature of the sCO2 flowing into the heater increases as turbine inlet temperature increases and system pressure decreases. Much of the space in this figure is in the vicinity of conditions necessary to achieve a low reactor inlet temperature. AREVA specifies a reactor inlet temperature of 325 °C. However, this number is dependent upon the approach temperature of the IHX at the cold point of the Helium and the reactor inlet temperature was arrived at under the assumption of a steam power conversion system. The use of a Brayton cycle will affect the approach temperature due to the relative temperature-enthalpy curves of the primary coolant and the power conversion working fluid. Thus, the assumptions in this report do not allow for such a low reactor inlet temperature.

Table 4 Table of values used in the trade study for system pressure and turbine inlet temperature.

Parameter	Units	Value
Main compressor inlet temperature	°C	32
Main compressor inlet pressure	MPa	7.7
Compressor discharge pressure	MPa	variable
Turbine inlet temperature	°C	variable
Low temp recuperator pinch temp at cold end	Δ°C	10
High temp recuperator pinch temp at cold end	Δ°C	20
Turbine efficiency	-	0.90
Main compressor efficiency	-	0.80
Recompressor efficiency	-	0.80
Fractional pressure drop through each major component	ΔP/P	0.01
Electric Power Output	MWe	250

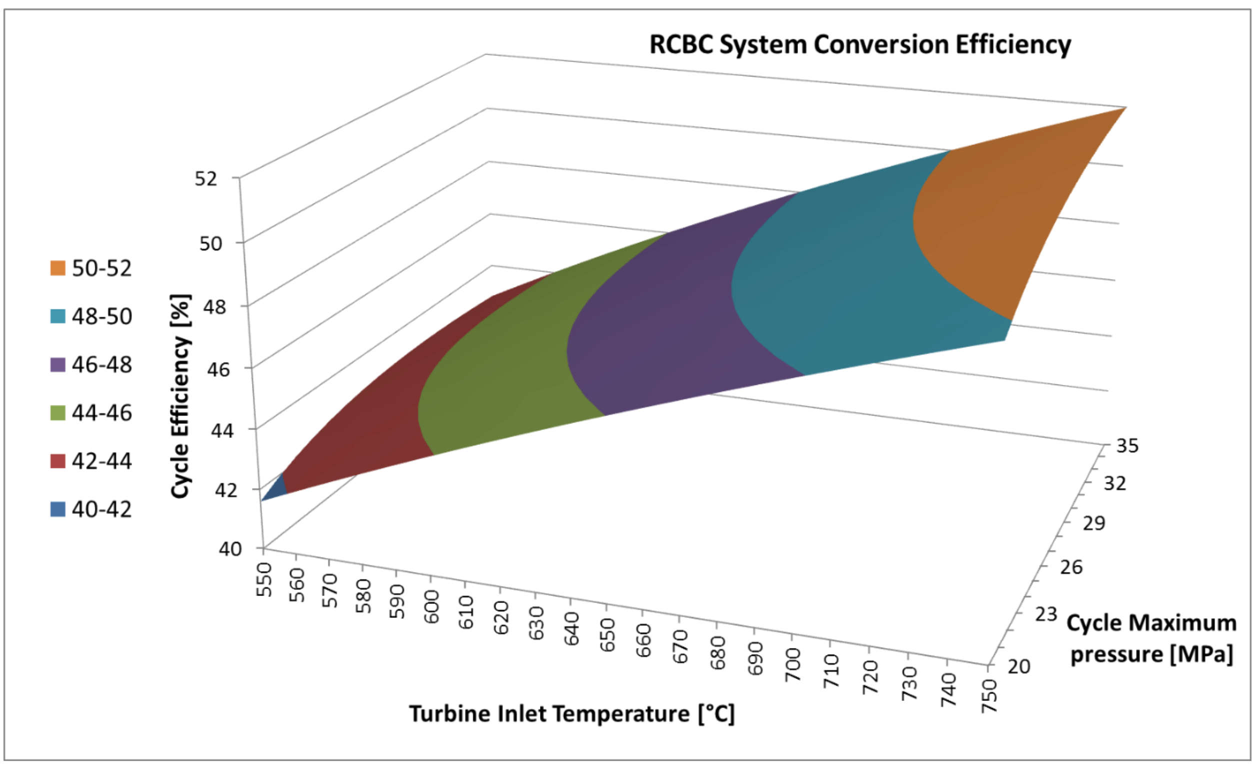

Figure 5 Effects of system pressure and turbine inlet temperature on conversion efficiency.

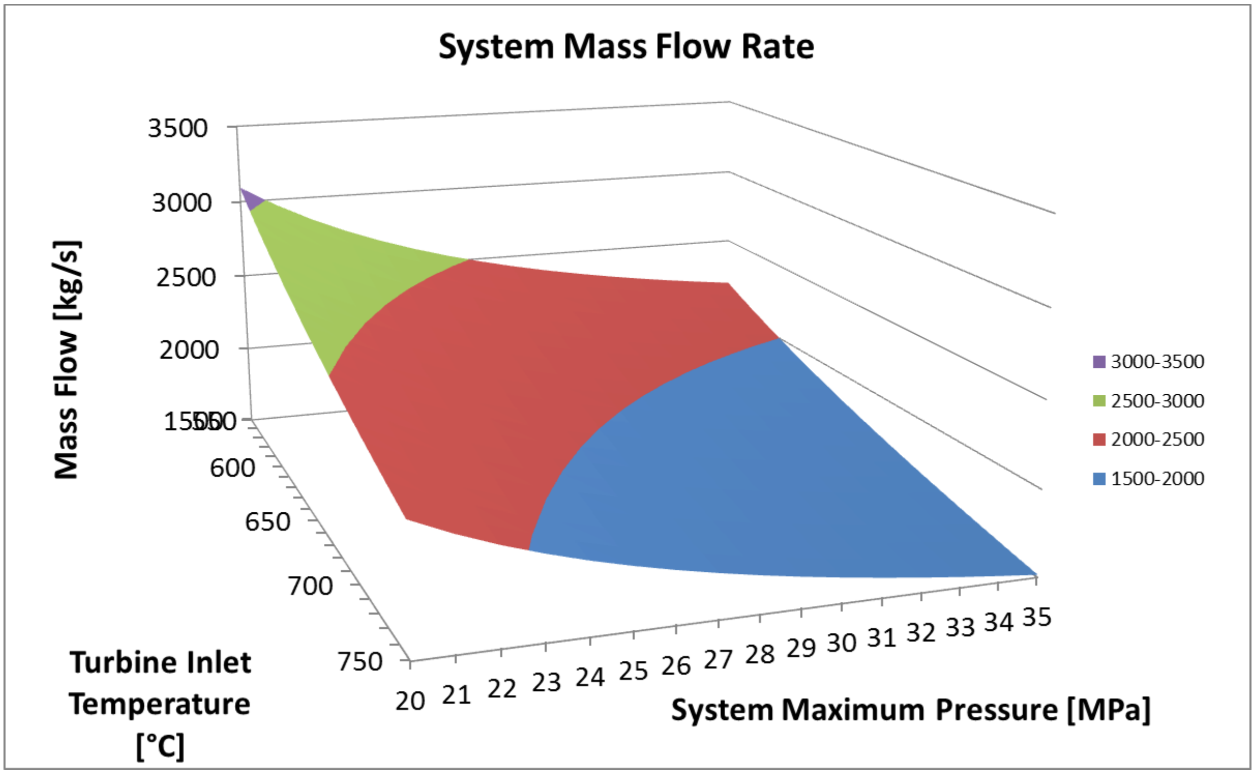

Figure 6 Effects of system pressure and turbine inlet temperature on system mass flow rate.

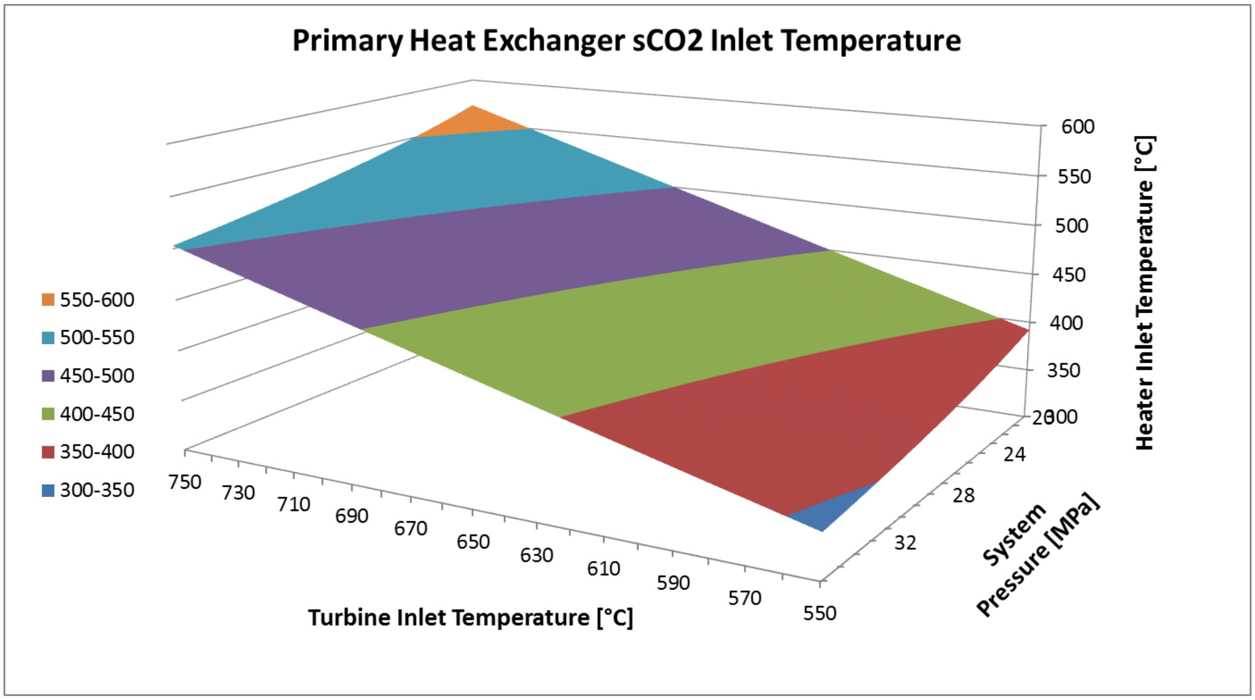

Figure 7 Power cycle fluid temperature at heater inlet.

Brayton Cycle Control Parameter Effect on HTGR Power and Helium Flow Rate

Utilizing the output from the RCBC trade study, reactor power and Helium flow rate were calculated. In order to perform this calculation, an assumption had to be made for the approach temperature for the IHX. For this initial study, it was assumed that the difference between the helium temperature and the CO_2 temperature was 15 °C at both ends of the IHX. For a more detailed study, a model of the IHX utilizing Pinch Point analysis would be more appropriate. Figures 8 and 9 present the Reactor Power Level and the Helium mass flow rate required to achieve the values in the thermodynamic trade study.

As expected, the required reactor power level decreases strongly with turbine inlet temperature and less so with cycle maximum pressure. This can also be seen by looking at Figure 5 (RCBC Cycle Efficiency), since Reactor Power Level is inversely proportional to cycle efficiency under the assumption of a constant IHX effectiveness.

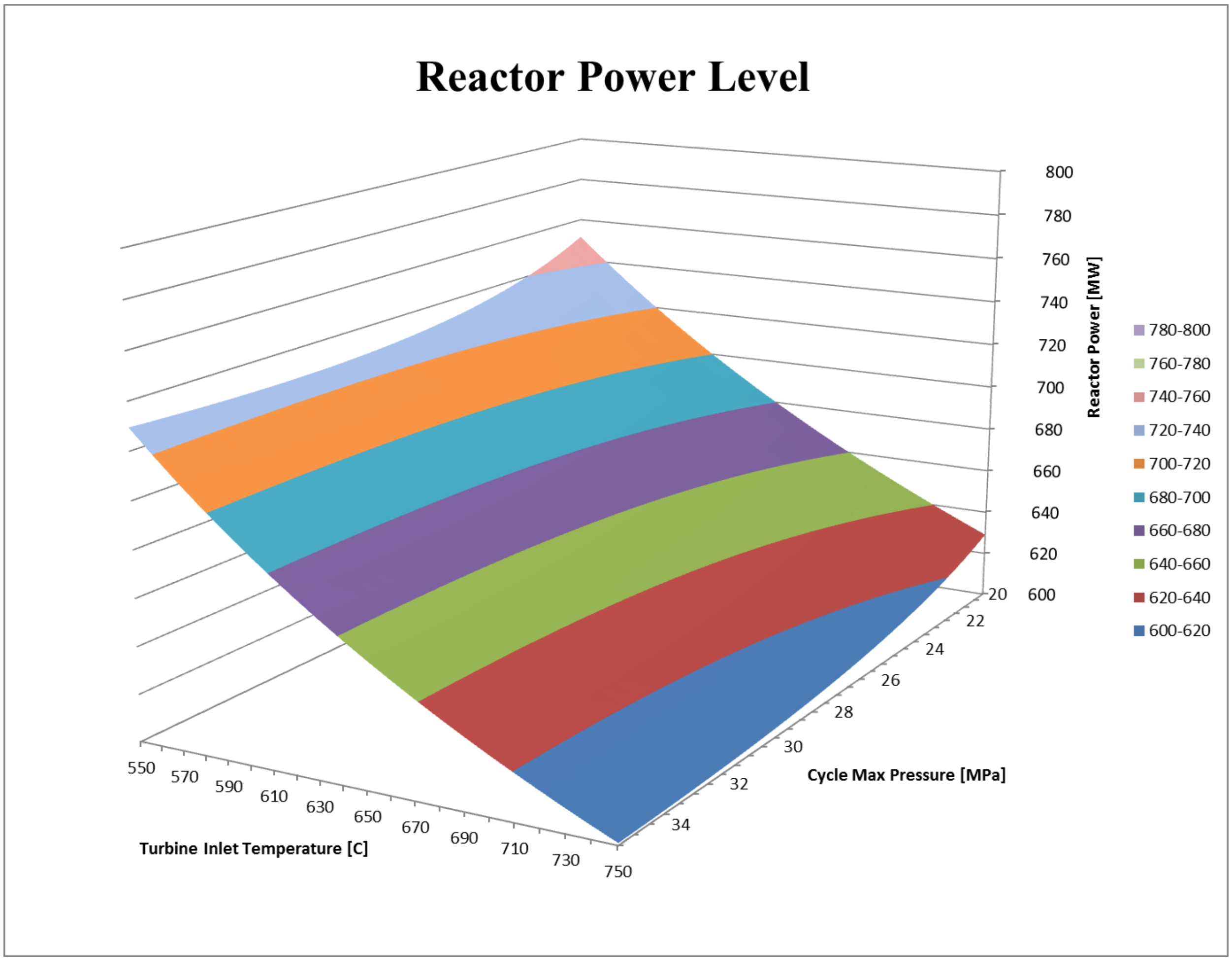

Figure 8 Reactor power level required to achieve 250 MWe, as a function of turbine inlet temperature and cycle maximum pressure.

Reactor coolant flow rate is a monotonically increasing function of reactor power. However, the two are not directly proportional over the temperature and pressure ranges of interest. This is due to the value of the specific enthalpy changing over those ranges also. The Helium flow rate as a function of turbine inlet temperature and cycle maximum pressure is shown in figure 9.

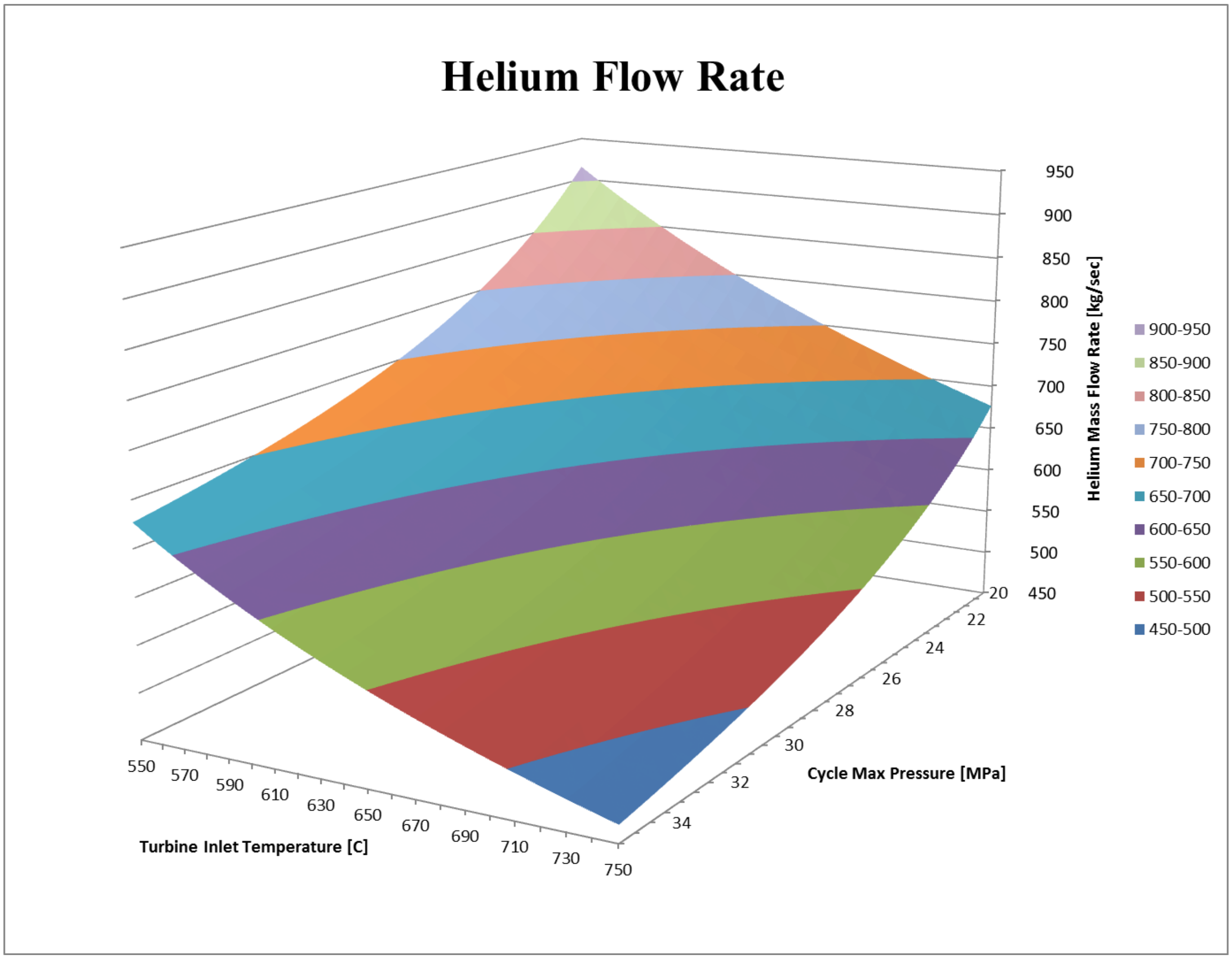

Figure 9 Primary coolant (Helium) mass flow rate vs. turbine inlet temperature and cycle maximum pressure.

4. MATERIALS CONSIDERATIONS

As part of the study, Sandia conducted a literature review to assess the current state of materials research pertaining to an HTGR being coupled to a sCO_2 Brayton cycle. Temperature and pressure assumptions erred on the side of the extreme. The assumptions for the study included the following.

1. Helium conditions from the HTR are at 800°C (1073K) at 6MPa.
2. Typical gas impurities are: CO/CO_2 (0.5-7.5Pa), CH_4 (0.5-2.5Pa), H_2O (<0.1Pa), H_2 (10-50Pa), and N_2(<0.5Pa) [5,6]. Sources for impurities listed below.
    a. CO/CO_2: oxidation of graphite/carbon by oxygen from air leakages and Boudouard reaction.
    b. CH_4: radiolytic graphite-hydrogen reaction at low temperatures
    c. H_2O: desorbed water in graphite reflectors, fresh fuel, etc.
    d. H_2: permeation from other circuits
    e. N_2: air leakages
3. sCO_2 cycle is at roughly 700°C (973K) with a pressure of 30MPa
    a. Fluid purity levels are unknown at this time and indications from literature are discussed.

Helium Corrosion

Helium is a noble gas and it is expected that there would be no compatibility issues with this fluid. Impurity content within the gas has been shown to be the primary driver for materials incompatibility [5-9]. Three temperature ranges of interest were identified with regards to materials: 350-600°C, 600-800°C, and 800-1000°C [3].

Within the range of 350-600°C decarburization of carbon steels is a concern and they should not be used above 370°C [3] . 2 ¼ Cr/Mo or 9-12% Cr steels should be used above 370°C, as Cr content should allow formation of protective chrome oxides (chromia) that prevents decarburization. Interested readers should refer to [3] for more information.

At the 600-800°C range four features were observed: chromia formation, internal oxidation of aluminum, decarburization (condition dependent), and carburation (condition dependent). Graham found that 100μm was the maximum depth of affected material over 5.7 years of exposure. Corrosion rates of <25μm/year is considered outstanding material resistance [8]. It should be noted that behavior is highly dependent upon gas chemistry and actual chemistries should be evaluated. Shindo suggested that carbon activity and oxygen content are primary indicators of materials performance (Figure 10). While observed rates of corrosion appear to be sufficiently low over this temperature range, mechanisms proceed rapidly above 800°C.
Above a critical temperature, which is alloy dependent (~900°C [3,7]), the alloy decarburizes/carburizes depending on the chemical regime. Chemical regime can be identified by monitoring the ratio of CH_4/H_2O. High ratio values of (excess carbon) favor regions IV and V in Figure 10 (i.e. formation of metal carbides and continuous carburization), while low ratio values (excess water) favor regions II and III (formation of metal oxides and decarburization) [3, 6]. Practical implications of these are that

decarburization can result in reduced creep strength, while carburization may cause a decrease in ductility. The upper temperature range should be evaluated for corrosion performance.

sCO_2 Corrosion

sCO2 corrosion studies have been performed over the last several years under various conditions (pressure/temperature) with standard materials [9-19]. Main conclusions are that corrosion increases with temperature for short term exposures, but long duration exposures are still needed [17]. Furthermore, austenitic steels should be used above 650°C, due to poor corrosion performance of ferritic-martensitic steels [19], To date it is unclear how pressure influences corrosion rates [16,17] and to what extent impurity content will influence mechanism[16]. Carburization was observed in alloys starting at 550°C with rates increasing as a function of pressure [10] and temperature [20]. Formation of protective chrome oxide scales appeared to mitigate this behavior [20], but continues to be an outstanding area of investigation.

Insufficient data still exists with regards to materials selection. Depth of affected material is rarely reported, but could be extracted from literature with some effort. Choice of alumina vs. chromia forming alloys as a function of temperature is unclear, though data suggests chromia formers are better for temperatures around 650°C [17].

Mechanical Considerations

ASME B31.1 (Power Piping Code) and the Boiler and Pressure Vessel Code (BPV) code provides allowable stresses for materials up to 815°C and above (see Table 5). Based upon allowable stresses listed in both codes, as a function of temperature, minimum wall thicknesses are calculated per Equation 1. This minimum wall thickness **does not** include allowances for corrosion over the pipe lifetime – this must be added per variable *A* in Equation 1. The purpose here is for illustrating typical minimum wall thicknesses for seamless piping materials for use at high temperatures. Due to insufficient heat exchanger design, pipe wall thickness was used for illustration.

The maximum differential pressure between helium and sCO_2 is 24MPa (3.48ksi). This pressure was assumed to be an internal pressure source, as given in the ASME B31.1 code. It is worth noting three observations.

First, with regards to high temperature containment, alloy 740H is nearly two times stronger between temperatures of 650-790°C(1200-1400°F), however above this temperature range a drastic fall off in strength occurs (Figure 11), making alloy 230 and 617 better choices for temperatures approaching 815°C (1500°F). At the high temperatures, for the conditions used here, the internal diameter available for fluid flow is limited to ~40% of the D_o, while with 300 series alloys the internal diameter is only ~10% of D_o.

Second, as expected from Equation 1, wall thickness scales linearly with diameter (Figure 12). Trade studies between pipe diameter size and cost per mass of the material should be performed to best determine geometrical configuration and layout.

Third, during practical operation many failures occur due to creep failure (also called stress rupture). Creep is a time-dependent deformation that occurs at high temperatures while under constant stress. Allowable stress determinations are made by a 1% creep expansion over 100,000 hour of operation (11.4 years) [21]. Much of the code already accounts for creep making allowable stresses a conservative choice for use in design calculations.

Questions/Opportunities

- High temperature range of materials in He should be evaluated, based upon prototypic impurity content.
- Investigation of sCO_2 literature to determine metal loss as a function of condition (pressure, temperature).
- sCO_2 high temperature materials research is needed to identify typical impurity content in the cycle.
- sCO_2 high temperature testing is needed to understand if impurity content changes corrosion mechanisms.
- Assess HT heat exchanger configuration then perform finite element modeling to remove stress risers.
- Optimize cycle configuration based upon materials available in the code.

Table 5 High temperature materials from piping and BPV codes

Materials rated up to 815°C (1500°F)			
Common Name	**Location**	**Common Name**	**Location**
304H	Power Piping B31.1	617	BPVC, Sec II, Part D
316H	Power Piping B31.1	625	BPVC, Sec II, Part D
321H	Power Piping B31.1	HR-120	BPVC, Sec II, Part D
347H	Power Piping B31.1	RA 330	BPVC, Sec II, Part D
800	Power Piping B31.1	800	BPVC, Sec II, Part D
800HT	Power Piping B31.1	800HT	BPVC, Sec II, Part D
617	Power Piping B31.1	HR-160	BPVC, Sec II, Part D
556	Power Piping B31.1	556	BPVC, Sec II, Part D
Hastelloy X	BPVC, Sec II, Part D	253MA	BPVC, Sec II, Part D
RA 602	BPVC, Sec II, Part D	740H**	BPVC, Code Case 2702
230	BPVC, Sec II, Part D	310	BPVC, Sec II, Part D
300 stainless 'H' grades included in BPVC, **Limited to temperatures of 800°C (1472°F)			

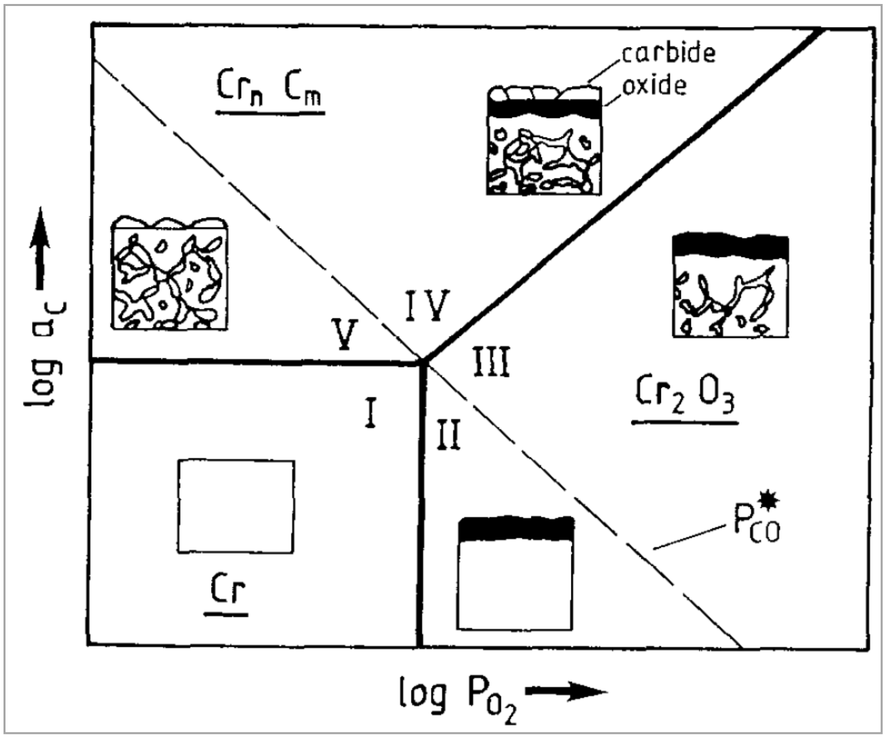

Figure 10 Suggested mechanisms of behavior of Cr based upon carbon activity (vertical axis) and partial pressure of oxygen (horizontal axis) [6]

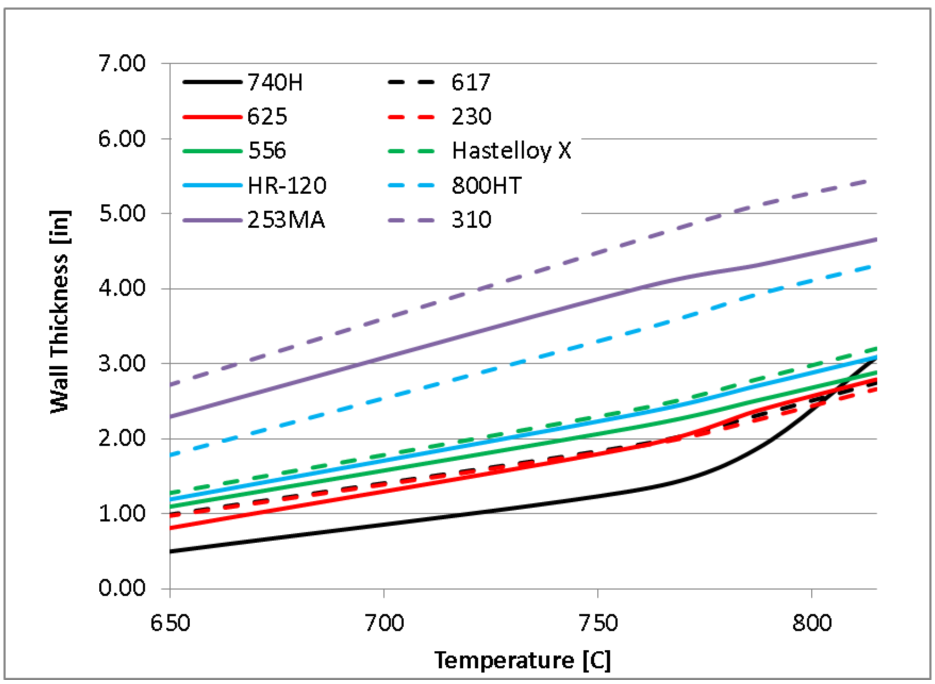

Figure 11 Wall thickness as a function of temperature for selected materials. (10" outer diameter with 24MPa internal pressure)

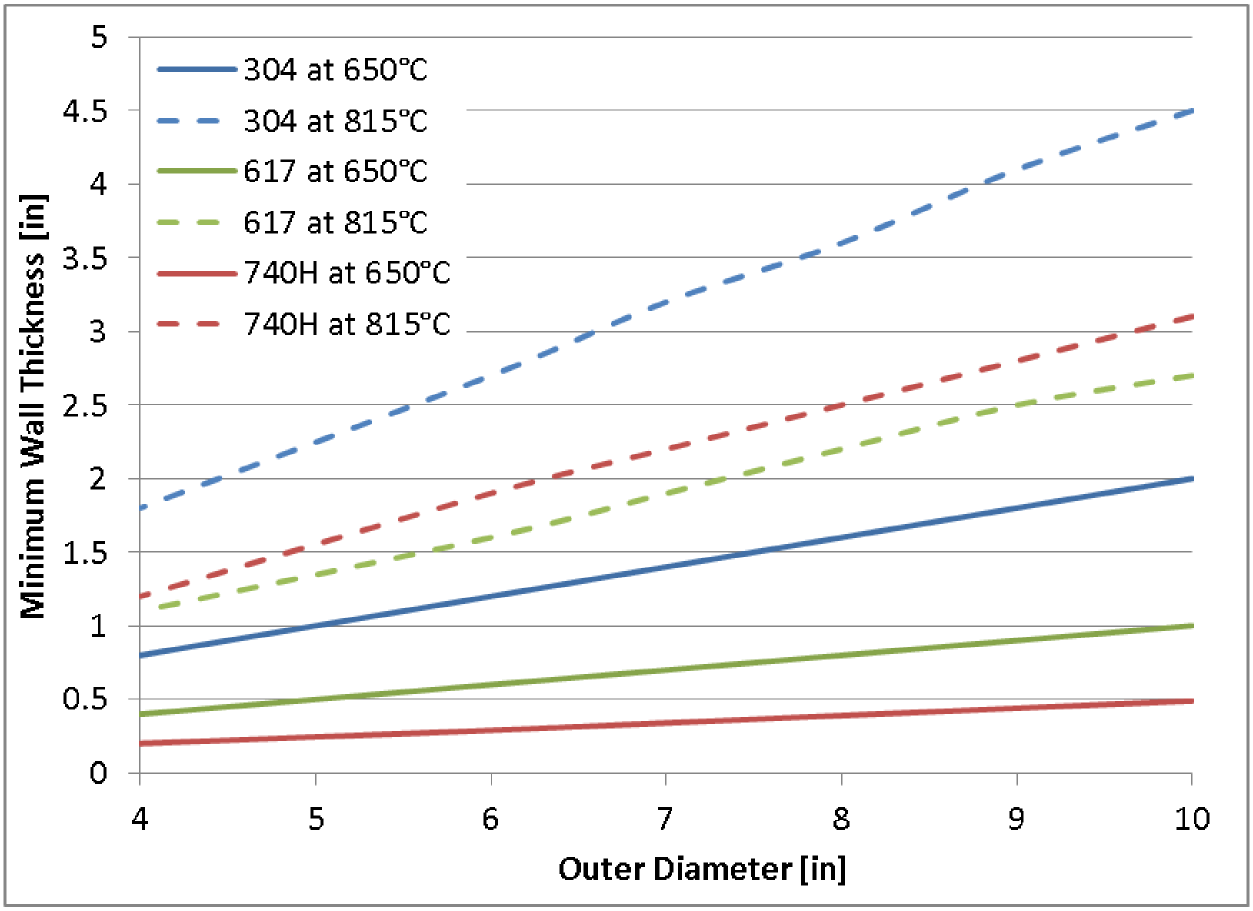

Figure 12 Wall thickness change as a function of diameter, temperature, and material at 24 MPa.

Minimum wall thickness calculation (Equation 7 in B31.1-2014):

$$t_m = \frac{PD_o}{2(SE + Py)} - A. \quad \text{Equation 1}$$

5. DRY HEAT REJECTION POTENTIAL[2]

Almost all thermoelectric power generation cooling is currently achieved via one of the following four arrangements.

1. Once-through Cooling – Water is withdrawn from a river, lake, or other natural water source, pumped through a condenser to cool/condense the steam exiting the turbine of a power conversion cycle, then returned to the natural water source. Little to no evaporation takes place. However, the discharged water has a higher temperature than the withdrawn water, thus contributing to some environmental effect.
2. Wet Cooling Tower – Wet cooling towers can be divided into two sub-categories:

[2] The content of this section is taken from a SAND report describing the work of a Laboratory Directed Research and Development project funded by Sandia National Laboratories. The report is listed in the References section as Reference #22.

a. Direct (Open Circuit) Wet Cooling – The water being used to cool the working fluid of the power conversion unit is passed through a cooling tower, making direct contact with the air being used to evaporate the cooling water. The water that is lost to evaporation is replaced with "makeup" water from the natural water source.
b. Indirect (Closed Circuit) Wet Cooling – The water being used to cool the working fluid of the power conversion unit is in a closed circuit and never makes direct contact with the air. Instead, water from the natural water source is passed over the outside of the piping that is used to recirculate the cooling water. Air is also made to pass over the freshwater supply, causing it to evaporate, thereby "indirectly" cooling the plant.

3. Dry Cooling Tower – The water being used to cool the working fluid of the power conversion unit is routed to a header, which then directs the hot fluid into a specially-designed water-to-air heat exchanger. Either forced or natural draft air is used to cool the water, which is recirculated to the plant. This type of cooling does not evaporate water, but it does decrease power conversion efficiency.
4. Hybrid Cooling Tower – A hybrid cooling tower combines both the wet and dry cooling tower concepts into one device. Typically, the portion of steam that is passed through the dry cooling circuit decreases as the ambient temperature increases. In this way, an optimum strategy can be developed that will minimize losses due to the decreased efficiency caused by dry cooling.

Dry heat rejection units are costly in three major ways. They are:

1. Installation costs are higher than wet cooling due to the need for more cooling towers.
2. Operation and maintenance costs are higher due to the hotel power needed to drive powerful fans for forced air cooling.
3. Plant efficiency is decreased due to the less efficient removal of waste heat.

SCO_2 Brayton cycles are much better matched, thermodynamically, to dry cooling than steam cycles. Steam cycles must reject waste heat at a constant temperature. This limits the temperature rise of the air that is used to remove the heat, dependent upon the pinch value used for the condenser that is used to transfer the heat. Brayton cycles, on the other hand, reject heat over a range of temperatures, allowing the air to be heated to a much higher temperature, thereby decreasing the flow rate of air needed. Figure 14 illustrates this concept.

Recent studies have suggested that the installation costs of dry heat rejection technology for sCO_2 Brayton cycles can be comparable to the installation costs of wet cooling technology for steam cycles. Figure 15 presents this concept.

Further work in this area could potentially result in major reductions in dry heat rejection costs for nuclear power plants, and indeed, for all thermoelectric power generation. Approximately 1/3 of the Earth is considered arid land. Making dry heat rejection competitive with wet cooling would make the production of energy throughout the world easier and potentially less expensive.

Some potential areas with high payoff include heat exchanger development for sCO_2 to air, how to take advantage of natural circulation to minimize power required for forced air, and design of a natural draft cooling system specifically for a Brayton cycle.

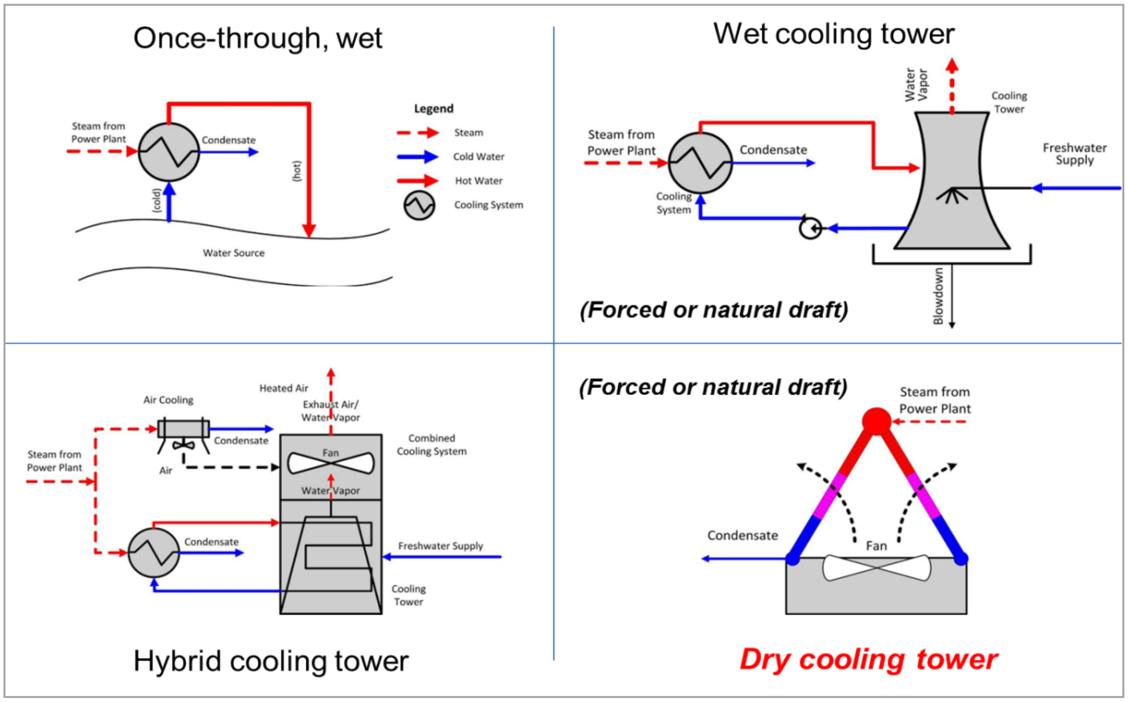

Figure 13 Illustration of four basic types of cooling options for large-scale power generation [Middleton, et al 2015].

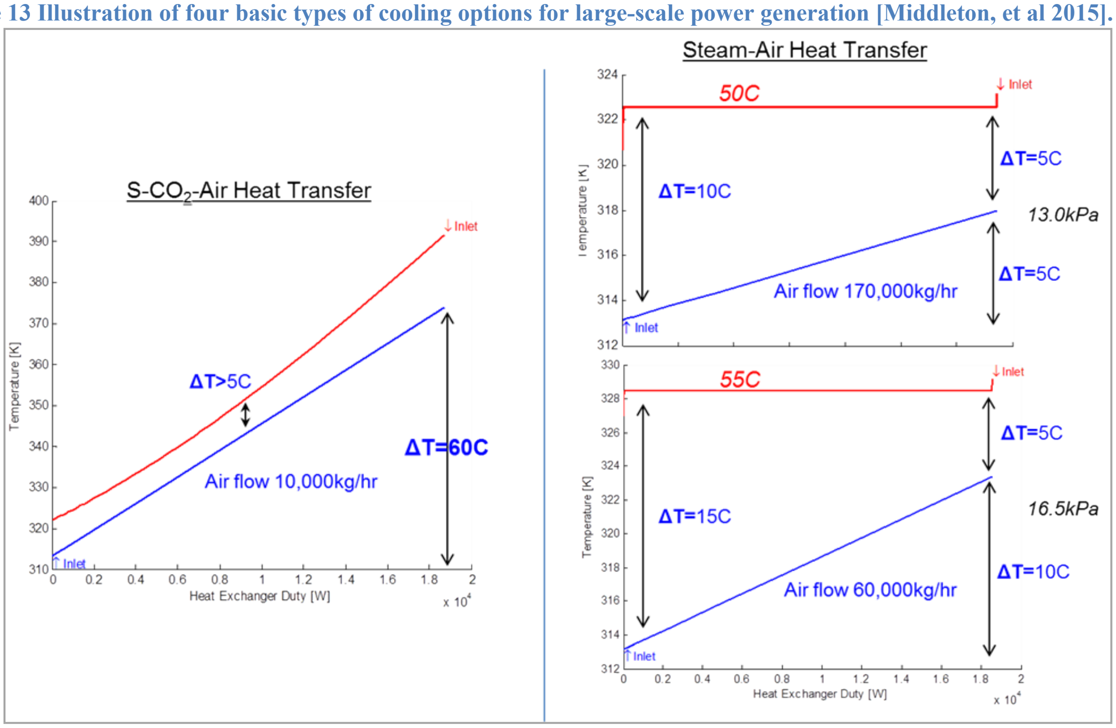

Figure 14 Comparison of air flow rate required for sCO2 Brayton and steam Rankine cycles [Middleton, et al 2015].

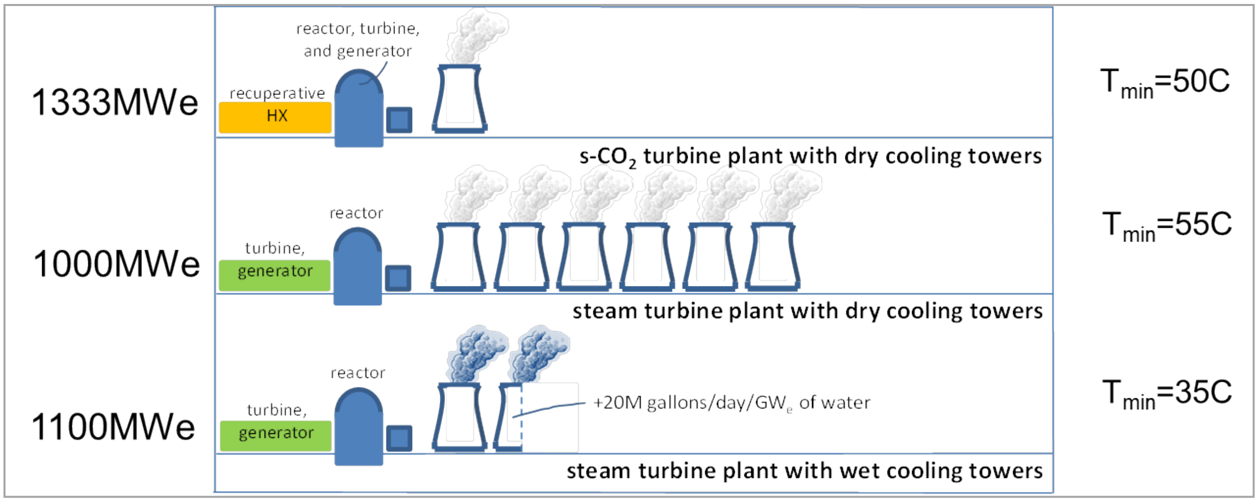

Figure 15 Comparison of number of cooling towers needed for various power conversion cycles [Middleton, et al 2015].

6. SUMMARY

A preliminary trade study was performed that assessed the consequences of coupling a supercritical CO_2 Brayton cycle to a Helium-cooled High Temperature Gas Reactor. The two parameters that were found to be the most important in determining the operational characteristics of the cycle are the turbine inlet temperature and the cycle maximum pressure. Power conversion efficiency, and therefore other parameters of interest, were all found to be most strongly dependent upon turbine inlet temperature and less so on cycle maximum pressure. The parameters that were studied were:

- CO_2 mass flow rate,
- IHX sCO_2 inlet temperature,
- Reactor power level, and
- Helium mass flow rate.

A literature review of materials considerations was also conducted. No glaring issues that would stop the use of a sCO_2 Brayton cycle from being coupled to a Helium-cooled HTGR were discovered. The review resulted in a list of items that need further work. This list includes the following.

- High temperature range of materials in He should be evaluated, based upon prototypic impurity content.
- Investigation of sCO_2 literature to determine metal loss as a function of condition (pressure, temperature).
- sCO_2 high temperature materials research is needed to identify typical impurity content in the cycle.
- sCO_2 high temperature testing is needed to understand if impurity content changes corrosion mechanisms.
- Assess HT heat exchanger configuration then perform finite element modeling to remove stress risers.
- Optimize cycle configuration based upon materials available in the code.

A review of some work related to dry heat rejection of a sCO_2 Brayton cycle was also conducted. This work is in its early stages and further work needs to be conducted in this area. Some areas that need to be considered are:

- Heat exchanger development for sCO_2 to air,
- How to take advantage of natural circulation to minimize power required for forced air, and
- Design of a natural draft cooling system specifically for a Brayton cycle.

REFERENCES:

1. Todreas, Neil E. and Mujid S. Kazimi, *Nuclear Systems I, Thermal Hydraulic Fundamentals*, Hemisphere Publishing Corporation, USA, 1990.
2. AREVA HTGR, High Temperature Gas-cooled Reactor, Information Kit, March, 2014.
3. L. W. Graham, "HIGH TEMPERATURE CORROSION IN IMPURE HELIUM ENVIRONMENTS," High temperature technology, vol. 3, pp. 3-14, 1985.
4. G. Menken, R. Nieder, L. W. Graham, H. Schuster, and W. Thiele, "REVIEW OF THE GAS/METAL INTERACTIONS IN HTR HELIUM UP TO 950 degree C," in Gas-Cooled Reactors Today, Proceedings of the Conference. Volume 4: Papers, Discussion, Closing Address, Corrigenda, Bristol, Engl, 1982, pp. 185-190.
5. [H. J. Christ, U. Kuenecke, K. Meyer, and H. G. Sockel, "HIGH TEMPERATURE CORROSION OF THE NICKEL-BASED ALLOY INCONEL 617 IN HELIUM CONTAINING SMALL AMOUNTS OF IMPURITIES," Materials science and engineering, vol. 87, pp. 161-168, 1986.
6. M. Shindo, W. J. Quadakkers, and H. Schuster, "CORROSION BEHAVIOUR OF HIGH TEMPERATURE ALLOYS IN IMPURE HELIUM ENVIRONMENTS," Journal of Nuclear Materials, vol. 140, pp. 94-105, 1986.
7. F. Rouillard, C. Cabet, K. Wolski, A. Terlain, M. Tabarant, M. Pijolat, et al., "High temperature corrosion of a nickel base alloy by helium impurities," Journal of Nuclear Materials, vol. 362, pp. 248-252, 2007.
8. D. A. Jones, Principles and prevention of corrosion. Upper Saddle River, NJ: Prentice Hall, 1996.
9. G. Cao, V. Firouzdor, K. Sridharan, M. Anderson, and T. R. Allen, "Corrosion of austenitic alloys in high temperature supercritical carbon dioxide," Corrosion Science, vol. 60, pp. 246-255, 2012.
10. F. Rouillard, G. Moine, M. Tabarant, and J. C. Ruiz, "Corrosion of 9Cr Steel in CO2 at Intermediate Temperature II: Mechanism of Carburization," Oxidation of Metals, vol. 77, pp. 57-70, 2012/02/01 2012.
11. F. Rouillard, F. Charten, and G. Moine, "Corrosion behavior of different metallic materials in supercritical carbon dioxide at 550C and 250 bars," Corrosion, vol. 67, 2011.
12. P. J. Roman, K. Sridharan, T. R. Allen, J. J. Jelinek, G. Cao, and M. Anderson, "Corrosion study of candidate alloys in high temperature, high pressure supercritical carbon dioxide for Brayton cycle applications," in Corrosion 2013, March 17, 2013 - March 21, 2013, Orlando, FL, United states, 2013.
13. (1974). Corrosion of steels in carbon dioxide. Available: http://www.icevirtuallibrary.com/content/book/102142.
14. I. G. Wright, B. A. Pint, J. P. Shingledecker, and D. Thimsen, "Materials considerations for supercritical CO2 turbine cycles," in ASME Turbo Expo 2013: Turbine Technical Conference and Exposition, GT 2013, June 3, 2013 - June 7, 2013, San Antonio, TX, United states, 2013.

15. V.-A. Glezakou, L. X. Dang, and B. P. McGrail, "Spontaneous Activation of CO2 and Possible Corrosion Pathways on the Low-Index Iron Surface Fe(100)," The Journal of Physical Chemistry C, vol. 113, pp. 3691-3696, 2009/03/05 2009.
16. M. H. A. K. Sridharan, G. Cao, J.J. Jelinek, V. Firouzdor, and T.R. Allen, "Corrosion testing of materials in high temperature supercritical carbon dioxide environment," in Supercritical CO2 power cycle symposium, Boulder, CO, 2011.
17. B. A. Pint and J. R. Keiser, "Initial Assessment of Ni-Base Alloy Performance in 0.1MPa and Supercritical CO2," JOM, vol. 67, pp. 2615-2620, 2015.
18. L.-F. He, P. Roman, B. Leng, K. Sridharan, M. Anderson, and T. R. Allen, "Corrosion behavior of an alumina forming austenitic steel exposed to supercritical carbon dioxide," Corrosion Science, vol. 82, pp. 67-76, 5// 2014.
19. L. Tan, M. Anderson, D. Taylor, and T. R. Allen, "Corrosion of austenitic and ferritic-martensitic steels exposed to supercritical carbon dioxide," Corrosion Science, vol. 53, pp. 3273-3280, 2011.
20. H. E. McCoy, "Type 304 Stainless Steel vs Flowing CO2 At Atmospheric Pressure and 1100-1800F," Corrosion, vol. 21, pp. 84-94, 1965/03/01 1965.
21. D. French. (1991, Creep and Creep Failures. BULLETIN Available: http://www.nationalboard.org/Index.aspx?pageID=181.
22. Middleton, Bobby D., Salvador Rodriguez, and Matthew Carlson, "Design, Construction, and Operation of a Supercritical Carbon Dioxide Loop for Investigation of Dry Cooling and Natural Circulation Potential for Use in Advanced Small Modular Reactors Utilizing sCO_2 Power Conversion Cycles," SAND2015-10092, November, 2015.

DISTRIBUTION

External

1 Hans Gougar
Idaho National Laboratory hans.gougar@inl.gov (electronic copy)

Internal

1	MS0721	Susan Pickering	6200 (electronic copy)
1	MS0736	Evaristo Bonano	6220 (electronic copy)
1	MS1136	Gary Rochau	6221 (electronic copy)
1	MS1136	Bobby Middleton	6221 (electronic copy)

Housekeeping

1	MS0899	Technical Library	9536 (electronic copy)

Sandia National Laboratories